

Decoding scrambled quantum information that was never encoded: An experimental demonstration

Yi-Te Huang,^{1, 2, 3} Siang-Wei Huang,^{1, 2} Jhen-Dong Lin,^{1, 2} Adam Miranowicz,^{3, 4} Neill Lambert,³ Guang-Yin Chen,⁵ Franco Nori,^{3, 6, *} and Yueh-Nan Chen^{1, 2, 7, †}

¹*Department of Physics, National Cheng Kung University, Tainan 701401, Taiwan*

²*Center for Quantum Frontiers of Research and Technology (QFort), Tainan 701401, Taiwan*

³*RIKEN Center for Quantum Computing, RIKEN, Wakoshi, Saitama 351-0198, Japan*

⁴*Institute of Spintronics and Quantum Information, Faculty of Physics and Astronomy, Adam Mickiewicz University, 61-614 Poznań, Poland*

⁵*Department of Physics, National Chung Hsing University, Taichung 402202, Taiwan*

⁶*Physics Department, The University of Michigan, Ann Arbor, Michigan 48109-1040, USA.*

⁷*Physics Division, National Center for Theoretical Sciences, Taipei 106319, Taiwan*

Quantum information scrambling (QIS) describes the rapid spread of initially localized information across an entire quantum many-body system through entanglement generation. Once scrambled, the original local information becomes encoded globally, inaccessible from any single subsystem. In this work, we introduce a protocol that enables information scrambling into the past, allowing decoding even before the original information is generated. This protocol is achieved by simulating a closed timelike curve—a theoretical construct in which particles can traverse backward in time—using postselection methods. Remarkably, the postselected outcome corresponds to a paradox-free trajectory that enables consistent time travel and reliable information recovery. Furthermore, the success probability is governed by out-of-time-ordered correlations, which is a standard measure of QIS. We present a quantum circuit design and experimentally implement our protocol on cloud-based Quantinuum and IBM quantum processors. Our approach illuminates a unique quantum task: retrieving information encoded in the future without altering the past.

INTRODUCTION

Quantum information scrambling (QIS) arises from strong interactions in a many-body system [1–3]. Such dynamics rapidly correlates local information and generates many-body entanglement across all possible degrees of freedom within the global system [3–15]. This delocalization process in many-body physics is typically characterized by the decay of the out-of-time-order correlator (OTOC) [1, 2] and has sparked growing interest in various fields, such as quantum chaos [14–27], black hole thermalization and information problems [28–39], quantum collision models [40–42], quantum computing and error correction [43–45].

Local information can be encoded into a global system by utilizing QIS. In a scrambled system, the information becomes dispersed and inaccessible via local measurements due to many-body entanglement. The robustness of recovering the original quantum information depends on the strength and structure of this entanglement [43, 46]. Remarkably, it is possible to recover the information even when parts of the system are damaged or lost. For instance, if the scrambled state is damaged by a local measurement but this damage does not affect the useful information encoded in the entanglement correlations, one can still recover the original information [44, 46].

Another example is when a quantum state is thrown into a black hole, characterized by strong scrambling dynamics, and the information is believed to irretrievably disappear once it crosses the event horizon [28]. However, Ref. [28] proposed a thought experiment suggesting that it might be possible to probabilistically reconstruct the lost information from several emitted Hawking radiation photons from the black hole through a suitable decoding process. An efficient Yoshida-Kitaev probabilistic decoding protocol for this thought experiment was proposed [47], with some extended scenarios [48–50] experimentally demonstrated [51–54]. Such decoding protocol can also be considered postselected quantum teleportation. The preparation of Einstein-Podolsky-Rosen (EPR) pairs and the postselection of the measurement outcomes are necessary for the original state (information) to be successfully teleported (decoded) in their protocol.

While the Yoshida-Kitaev probabilistic decoding protocol has been widely adopted to characterize QIS, the physical intuition behind its essential ingredients, particularly the use of EPR pair preparation and postselection, has remained unclear. In this work, we clarify their role by drawing a parallel with the concept of postselected closed timelike curves (PCTCs) [55, 56].

A closed timelike curve (CTC) is a hypothetical concept in general relativity that describes a worldline in spacetime looping back on itself, allowing a particle to return to and interact with its own past [57, 58]. This idea suggests the possibility of time travel and may raise some paradoxes [59]. PCTCs enable a specific formulation that combines CTCs with quantum mechanics based on quantum teleportation and postselection [55, 56], which

* fnori@riken.jp

† yuehnan@mail.ncku.edu.tw

can be simulated on quantum processors [60–62]. The postselection step introduces nonlinear effects that enforce the Novikov self-consistency principle [63], which dictates that only logically self-consistent events can occur. Paradoxical outcomes are assigned zero probability, and the success probability of time travel corresponds to the conditional probability of such consistent events. Beyond foundational insights into quantum gravity [64–66], the PCTC framework has found applications in quantum information processing [67–70] and quantum metrology [71, 72].

In this work, we propose a PCTC-inspired protocol to transmit scrambled (encrypted) quantum information into the past. Remarkably, we show that *this encrypted message can be decoded even before the original information is generated*. We show that our protocol is operationally equivalent to the Yoshida-Kitaev probabilistic decoding protocol [47, 50]. Within our formulation, the roles of the EPR pair and postselection become physically transparent: they serve as the essential ingredients for constructing a paradox-free PCTC [63], thereby enabling consistent and successful information recovery in the past.

The protocol is quantified by the fidelity between the original state prepared in the future and the decoded state in the past. Furthermore, the decoding fidelity depends on the success probability of time travel through a PCTC. Nevertheless, this success probability depends on the strength of QIS, characterized by the decay of the average value of the OTOC. Therefore, sufficiently strong scrambling dynamics guarantees that the original information to be perfectly decoded (with unity fidelity). Finally, we demonstrate our decoding protocol using a four-qubit quantum circuit and then implement it on Quantinuum H1-1 trapped-ion quantum processor [73].

RESULTS

Recovering scrambled information via postselected closed timelike curves

We introduce a protocol for recovering scrambled information from the future, as illustrated schematically in Fig. 1. Our protocol includes three main steps: (1) encoding quantum information using QIS, (2) time-travel part of the encoded information into the past via a PCTC, and (3) decoding the original information.

We begin with Alice (A), who prepares an arbitrary pure quantum state $|\psi\rangle$ with Hilbert space dimension d_A at time T_1 . As time progresses from T_1 to T_2 , system A interacts with a chronology-respecting many-body system H, and the global evolution of this interaction is described by an encoding unitary operator $U_{\text{encode}} = U_{\text{AH} \rightarrow \text{HE}}$. Here, U can also be called a *scrambler*, and the subscript labels the input subsystems (A and H) and output subsystems (H and E) of the operator. Note that the state of system H at T_1 will be discussed later. The

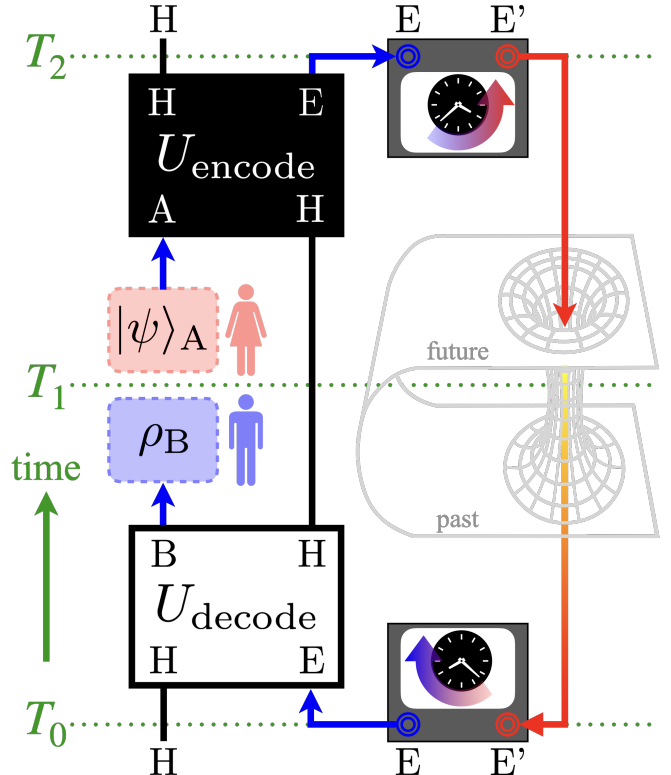


FIG. 1. **Schematic illustration of the decoding protocol.** The black solid lines depict the timeline of the many-body system H going forwards. The blue (red) arrows depict the timeline of a portion of the encoded information E (E') going forwards (backwards). Starting at time T_1 , Alice (A) sends the information $|\psi\rangle$ into the scrambling unitary operator (scrambler) $U_{\text{encode}} = U_{\text{AH} \rightarrow \text{HE}}$, encoding the information in the joint system HE at T_2 . By projecting the state of joint system EE' into an EPR state, the temporal direction for E is reversed, causing it to travel backward in time from T_2 to T_0 . Because the state of system E and E' are initialized as an EPR state at T_0 , the temporal direction for E' is reversed again. The decoding unitary operator $U_{\text{decode}} = U_{\text{HE} \rightarrow \text{BH}}^\dagger$ allows Bob (B) to decode Alice's information solely from the portion of the encoded information carried in E at T_0 . Therefore, Bob obtains the state ρ before Alice prepares $|\psi\rangle$ at T_1 . The information is perfectly decoded if and only if the fidelity between $|\psi\rangle$ and ρ is unity.

quantum information $|\psi\rangle$ has become scrambled within the many-body entanglement of the joint system HE at T_2 . Here, the output system E represents a part of the encoded information with its Hilbert space dimension also equal to d_A .

Next, the temporal direction of system E is reversed at time T_2 , allowing it to travel back to T_0 (a time point before T_1) and then resume traveling forward in time. This is achieved by utilizing a PCTC, where we introduce a chronology-violating system E', depicted as the red curve in Fig. 1. If the initial state of E and E' at T_0 is a maximally entangled state, E' can be interpreted as a mirror of E that travels backward in time [55, 56]. Fur-

thermore, it is necessary to perform a projective (or selective) measurement on the joint system EE' at T_2 , and the measurement outcome must remain consistent with itself (the same state) at T_0 to obey the Novikov self-consistency principle [63]. Throughout this work, and without loss of generality, we consider the state of E and E' at T_0 to be prepared as an EPR pair [74], namely

$$|EPR\rangle_{EE'} = \frac{1}{\sqrt{d_A}} \sum_{i=0}^{d_A-1} |i\rangle_E \otimes |i\rangle_{E'}. \quad (1)$$

Therefore, an EPR projective measurement must be performed at T_2 , ensuring that the state of system E effectively travels backward to T_0 . We denote the success probability of time travel through the PCTC (preparing and measuring $|EPR\rangle_{EE'}$ at T_0 and T_2 , respectively) as $\mathcal{P}(\psi)$ for different state $|\psi\rangle$.

At time T_0 , a decoding operation $U_{\text{decode}} = U_{\text{HE} \rightarrow \text{BH}}^\dagger$ is applied to the joint system HE , and then Bob (B) subsequently receives a state ρ (generally represented as a density matrix) before T_1 . To demonstrate that the final decoding process requires only $U_{\text{HE} \rightarrow \text{BH}}^\dagger$ and the partially encoded information stored in E , we assume that the initial state of system H at T_0 is maximally mixed, which does not provide any additional information for the final decoding process. Finally, the fidelity between the states $|\psi\rangle$ and ρ quantifies the entire decoding protocol, namely

$$\mathcal{F}(\psi) = \langle \psi | \rho | \psi \rangle. \quad (2)$$

The original information prepared by Alice is perfectly decoded if and only if the fidelity equals unity.

Here, we prove that our decoding protocol is equivalent to the Yoshida-Kitaev probabilistic decoding protocol [47]. The proof under the diagrammatic notation is presented in Fig. 2, and a similar discussion for another protocol can also be found in Ref. [50].

In our protocol, the initial state of the many-body system H at T_0 is a maximally mixed state. However, the initial state in the Yoshida-Kitaev probabilistic decoding protocol is derived from an entangled EPR pair between system H and an auxiliary system H' , i.e., $|EPR\rangle_{HH'}$. Incorporating this constraint into our protocol, the final unnormalized state $|f(\psi)\rangle$, corresponding to the input quantum information $|\psi\rangle$ from Alice, can be expressed as

$$|f(\psi)\rangle_{\text{BHH}'} = \langle \text{EPR} |_{AB} U_{AH} U_{BH}^\dagger | \psi \rangle_A \otimes |EPR\rangle_{BB'} \otimes |EPR\rangle_{HH'}, \quad (3)$$

as shown in Fig. 2(b). Here, without loss of generality, we relabel the input system E (at time T_0), output system E (at time T_2), and the chronology-violating system E' as B , A , and B' , respectively. This relabeling is justified because, from the perspective of PCTCs, all these systems represent the same system that carries the information at different time points, or travels in different directions

in time. Additionally, for simplicity, we rearrange both the input and output Hilbert spaces into the same order as $\text{AHBB}'\text{H}'$ in the diagrammatic notation, as shown in Fig. 2(b). Note that although the diagrammatic notation of $|EPR\rangle_{HH'}$ in Fig. 2(b) appears as a single wire, it actually represents multiple EPR pairs shared between the corresponding subsystems of H and H' .

A key element of this proof is the following identity, which holds when an arbitrary local unitary U is applied to an EPR pair, namely

$$U_X \otimes \mathbb{1}_{X'} |EPR\rangle_{XX'} = \mathbb{1}_X \otimes U_X^T |EPR\rangle_{XX'}, \quad (4)$$

where the superscript T represents the transpose of an operator, and $\mathbb{1}$ is the identity operator. Thus, using the equality given in Eq. (4), we can replace the decoding unitary operation $U_{BH}^\dagger \otimes \mathbb{1}_{B'H'}$ with $\mathbb{1}_{BH} \otimes U_{B'H'}^*$ in Eq. (3), namely

$$|f(\psi)\rangle_{\text{BHH}'} = \langle \text{EPR} |_{AB} U_{AH} U_{B'H'}^* | \psi \rangle_A \otimes |EPR\rangle_{BB'} \otimes |EPR\rangle_{HH'}, \quad (5)$$

for which the corresponding diagrammatic notation is given in Fig. 2(c). After rearranging the input Hilbert space order to $\text{AHH}'\text{B}'\text{B}$ and the output Hilbert space order to $\text{HAB}'\text{H}'\text{B}$ in the diagrammatic notation [as shown in Fig. 2(d)], the unnormalized state $|f(\psi)\rangle$ is identical to the one presented in the Yoshida-Kitaev probabilistic decoding protocol [47]. Consequently, the normalized decoded state is given by

$$\rho_B = \frac{\text{Tr}_{HH'} [|f(\psi)\rangle \langle f(\psi)|_{\text{BHH}'}]}{\mathcal{P}(\psi)}, \quad (6)$$

where the success probability $\mathcal{P}(\psi)$ of time travel is expressed as

$$\mathcal{P}(\psi) = \langle f(\psi) | f(\psi) \rangle. \quad (7)$$

We emphasize that, in our protocol, the input state to the encoding scrambler U for system H must be the output from the decoding operation U^\dagger . This indicates that the decoding process must occur before the encoding process, unlike in the Yoshida-Kitaev probabilistic decoding protocol. Furthermore, their protocol requires generating multiple EPR pairs depending on the size of both systems H and E , whereas our protocol uses fewer entanglement resources. This is because we only require the preparation of a maximally mixed state for system H , and a single EPR pair between systems E and E' .

Furthermore, the product of the success probability $\mathcal{P}(\psi)$ and the fidelity $\mathcal{F}(\psi)$ is lower-bounded by d_A^{-2} [47], namely

$$\mathcal{P}(\psi) \mathcal{F}(\psi) \geq \frac{1}{d_A^2} \quad \forall \psi \quad (8)$$

(see Methods). This indicates that the original information is accurately decoded (with $\mathcal{F} \approx 1$) when the success probability is sufficiently low (with $\mathcal{P} \approx d_A^{-2}$) in the ideal case.

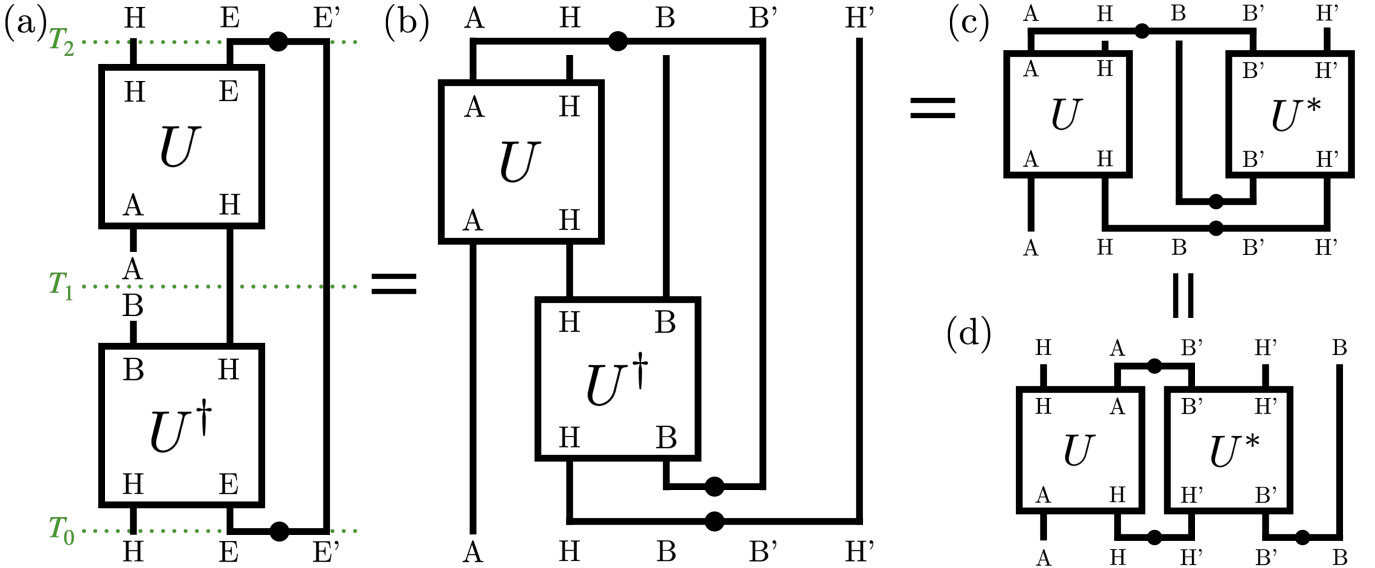


FIG. 2. **Proof of the equivalence of protocols using diagrammatic notation.** (a) The diagram of our decoding protocol, where time progresses from T_0 to T_2 in the laboratory's rest frame. Note that the black dot in the middle of the wire indicates a normalized EPR pair (scaled by $1/\sqrt{d}$). (b) We introduce the purification $|\text{EPR}\rangle_{HH'}$ for the initial state of the many-body system H , which is a maximally mixed state, with its reference system H' . For simplicity, we relabel the input system E (at time T_0), output system E' (at time T_2), and system E' as B , A , and B' , respectively. The equivalence between the diagrams in (b) and (c) follows from the properties of the EPR state, as described in Eq. (4). (d) Diagram obtained by rearranging the input and output Hilbert space order from the diagram in (c).

Quantum information scrambling and out-of-time-order correlators

Quantum information scrambling is typically characterized by the decay of the OTOC [1, 2], defined as

$$\mathcal{O}(W, V) \equiv \langle W^\dagger(t) V^\dagger W(t) V \rangle, \quad (9)$$

where W and V are initially commuting unitary and Hermitian operators acting on separate subsystems, and the operator $W(t) = U^\dagger W U$ is the time-evolved version of W in the Heisenberg picture according to the scrambling unitary operator U . When $t = 0$, the value of the OTOC $\mathcal{O}(W, V) = 1 \forall W$ and V because $W(0)$ commutes with V . As scrambling progresses, $W(t)$ ceases to commute with V as it becomes increasingly nonlocal, thereby leading to the rapid decay of the OTOC.

The average value of the OTOC in Eq. (9) can be directly calculated by the success probability $\mathcal{P}(\psi)$ of time travel in our decoding protocol [47]:

$$\mathcal{O}_{\text{avg}} = \iint dW dV \mathcal{O}(W, V) = \int d\psi \mathcal{P}(\psi) \quad (10)$$

(see Methods). Here, the double integral represents the Haar average over all unitary operators W and V on the corresponding subsystems, and the single integral averages over all initial states $|\psi\rangle$ in our protocol. The average success probability of time travel through the PCTC decreases as the average value of the OTOC decays.

Furthermore, one can observe that the average value of the OTOC decays to d_A^{-2} for the aforementioned perfect

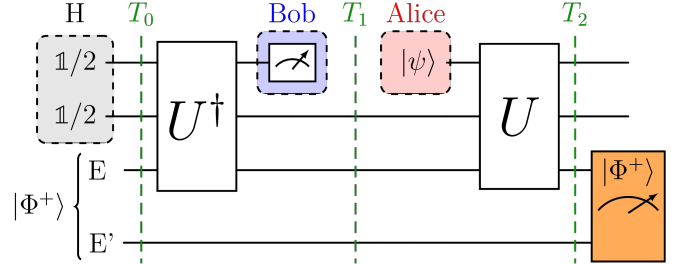


FIG. 3. **Experimental demonstration of the decoding protocol using a four-qubit quantum circuit.** Time progresses from T_0 to T_2 in the laboratory's rest frame. Initially, the system H is prepared as a two-qubit maximally mixed state, while the systems E and E' are initialized as $|\Phi^+\rangle = (|00\rangle + |11\rangle)/\sqrt{2}$, which is one of the Bell states. The three-qubit decoding operation U^\dagger is applied to decode the information stored solely in system E , and Bob performs quantum state tomography on qubit B before T_1 . After T_1 , Alice prepares the information $|\psi\rangle$ and encodes it using the scrambler U . To complete the decoding protocol, a Bell state measurement (BSM) is performed after T_2 , and Bob needs to postselect his results corresponding to the state $|\Phi^+\rangle$.

decoding case $[\mathcal{F}(\psi) = 1 \text{ and } \mathcal{P}(\psi) = d_A^{-2} \forall \psi]$. This indicates that *the unitary evolution U must generate sufficiently strong scrambling dynamics (which makes \mathcal{O}_{avg} decay to d_A^{-2}) so that the information $|\psi\rangle$ can be fully encoded through the many-body entanglement in the joint system HE at T_2 , and then perfectly decoded in the past*.

Experimental demonstration

As we mentioned above, although the existence of CTCs is still vague, one can probabilistically simulate it based on postselected quantum teleportation. Here, we demonstrate our decoding protocol using a four-qubit quantum circuit, shown in Fig. 3. The circuit is implemented using Quantinuum H1-1 quantum charge-coupled processor, which features 20 trapped-ion ($^{171}\text{Yb}^+$) qubits with all-to-all connectivity [73]. Note that the calibration data of this processor is presented in the Supplementary Information.

In the following, we explain the circuit in detail in the laboratory's rest frame (from T_0 to T_2). At time T_0 , system H is initialized as a two-qubit maximally mixed state $[(\mathbb{1}/2) \otimes (\mathbb{1}/2)]$, a uniform mixture of states in the computational basis. Thus, we uniformly prepare each of the two qubits in the state $|0\rangle$ or $|1\rangle$. Systems E and E' are initialized as a two-qubit EPR pair, as shown in Eq. (1) with $d_A = 2$:

$$|\Phi^+\rangle_{\text{EE}'} = \frac{1}{\sqrt{2}} (|0\rangle_E \otimes |0\rangle_{E'} + |1\rangle_E \otimes |1\rangle_{E'}), \quad (11)$$

which is a Bell state [74].

After applying the decoding operation U^\dagger to the joint system HE, we perform quantum state tomography (i.e., single-qubit Pauli measurements [74]) on qubit B before T_1 . To ensure the information is from the future, we reset qubit B and then prepare a pure quantum state $|\psi\rangle$ on the same qubit (which we rename qubit A after T_1). We emphasize that the state $|\psi\rangle$ is prepared freely, with no knowledge of the previous measurement results. We then apply the encoding scrambler U to encode the information within the joint system HE at T_2 . To complete the decoding protocol, a Bell state measurement is performed on the joint system EE' after T_2 , and we postselect the outcome corresponding to $|\Phi^+\rangle_{\text{EE}'}$ as in Eq. (11). Finally, we reconstruct the density matrix ρ from the postselected measurement results and calculate the fidelity $\mathcal{F}(\psi)$, given in Eq. (2), between the states ρ and $|\psi\rangle$, confirming that the quantum information encoded in the future has been successfully decoded from the past.

To characterize the nature of the scrambling dynamics, we repeat this protocol by encoding the six different initial states and two different scramblers: $|\psi\rangle \in \{|x_-\rangle, |x_+\rangle, |y_-\rangle, |y_+\rangle, |z_-\rangle, |z_+\rangle\}$, where $|x_\pm\rangle \equiv \frac{1}{\sqrt{2}}(|0\rangle \pm |1\rangle)$, $|y_\pm\rangle \equiv \frac{1}{\sqrt{2}}(|0\rangle \pm i|1\rangle)$, $|z_-\rangle \equiv |1\rangle$, and $|z_+\rangle \equiv |0\rangle$. For the scrambling unitary operator U , we consider the three-qubit Clifford scrambler proposed in Ref. [48]. Such scrambler, denoted as U_q , is capable of fully delocalizing arbitrary quantum information. The explicit matrix form

TABLE I. **Experimental results.** The decoding fidelity \mathcal{F} and the success probability \mathcal{P} of time travel for different initial states $|\psi\rangle$ under Clifford scrambler U_q . As shown in Eq. (10), the average value of the out-of-time-order correlator \mathcal{O}_{avg} equals the average value of $\mathcal{P}(\psi)$.

$ \psi\rangle$	$ x_-\rangle$	$ x_+\rangle$	$ y_-\rangle$	$ y_+\rangle$	$ z_-\rangle$	$ z_+\rangle$	Average
$\mathcal{F}(\psi)$	0.976	0.986	0.990	0.988	0.983	0.987	0.985
$\mathcal{P}(\psi)$	0.258	0.249	0.243	0.256	0.253	0.252	0.252

of this unitary operator is given by:

$$U_q = \frac{1}{2\sqrt{2}} \begin{pmatrix} 1 & 1 & 1 & -1 & 1 & -1 & -1 & -1 \\ 1 & -1 & 1 & 1 & 1 & 1 & -1 & 1 \\ 1 & 1 & -1 & 1 & 1 & -1 & 1 & 1 \\ -1 & 1 & 1 & 1 & -1 & -1 & -1 & 1 \\ 1 & 1 & 1 & -1 & -1 & 1 & 1 & 1 \\ -1 & 1 & -1 & -1 & 1 & 1 & -1 & 1 \\ -1 & -1 & 1 & -1 & 1 & -1 & 1 & 1 \\ -1 & 1 & 1 & 1 & 1 & 1 & 1 & -1 \end{pmatrix}, \quad (12)$$

and its circuit representation is given in Fig. 4. The success probability for an arbitrary state $|\psi\rangle$ under the scrambler U_q is $\mathcal{P}(\psi) = 0.25$. According to Eq. (8), this leads to an estimated fidelity of unity for any state $|\psi\rangle$, indicating perfect decoding.

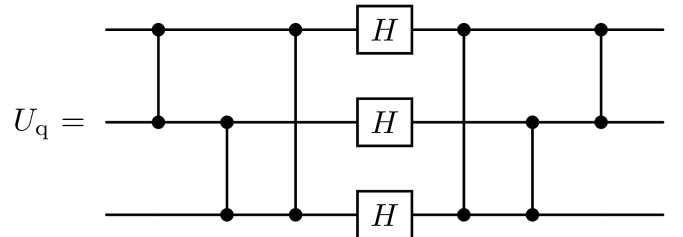


FIG. 4. **Circuit representation of the three-qubit Clifford scrambler.** This scrambling unitary operator includes six controlled-Z and three Hadamard (H) gates.

The experimental results, as shown in Table I, are obtained through 4,000 shots for each measurement procedure in the state tomography using the H1-1. We observe that the success probability $\mathcal{P}(\psi)$ of time travel approximately approaches $d_A^{-2} = 0.25$ for all initial states $|\psi\rangle$, which also means that $\mathcal{O}_{\text{avg}} \approx 0.25$ due to Eq. (10). Due to the strong QIS U_q , the decoding protocol succeeds with an average fidelity of 0.985. For the experimental results obtained from the IBM Quantum processor using different scrambling unitary operations, we refer the readers to the Supplementary Information.

CONCLUSION

We have proposed a protocol and experimentally demonstrated it on Quantinuum quantum processor,

leveraging QIS and PCTCs to transmit and decode encrypted quantum information from the future into the past. Although QIS delocalizes the original quantum information through many-body entanglement, we can still retrieve it by sending part of the scrambled information into the past. Time travel can be simulated through PCTCs, and its average success probability is directly related to the average value of OTOC in QIS. Notably, we show that the choice of the postselected outcome in our protocol is governed by the Novikov self-consistency principle: the outcome must be consistent with the state in which it was prepared in the past. Furthermore, we observe that the perfect decoding fidelity of our protocol requires strong QIS, which corresponds to a sufficiently low average value of the OTOC.

To substantiate our theoretical framework, we conducted a proof-of-principle experiment, highlighting the essential roles that QIS and PCTCs play in the success of decoding an encrypted message from the future. Importantly, our protocol preserves the causality of information [75]. Sending a secret to the past via PCTCs is like ouroboros, a serpent devouring its own tail. Any attempt to alter the past is a futile endeavor because whatever happened, happened.

Our work paves the way for several intriguing future research directions. First, integrating our protocol with existing quantum key distribution protocols could yield new cryptographic applications that leverage the time-travel aspects for enhanced secure communication. Second, our protocol allows the estimation of the average value of the OTOC for arbitrary QIS using only one additional entangled EPR pair. While our demonstration utilizes a three-qubit scrambler, exploring more complex scrambling dynamics could enhance the understanding of the relationship between the decoding fidelity and dif-

ferent types of QIS, potentially optimizing the protocol further. Finally, our protocol establishes a connection between QIS and PCTCs, exploring insights related to black holes, wormholes, and time travel.

METHODS

A lower bound for the product of the PCTC success probability and decoding fidelity

We demonstrate that the product of the PCTC success probability [\mathcal{P} in Eq. (7)] and the decoding fidelity [\mathcal{F} in Eq. (2)] in our decoding protocol is lower-bounded by d_A^{-2} for an arbitrary encoded state $|\psi\rangle$. Here, d_A denotes the Hilbert space dimension of the original input quantum information $|\psi\rangle$ from Alice. Note that a similar proof can also be found in Ref. [47]. We begin by substituting Eq. (6) into Eq. (2) and multiplying by $\mathcal{P}(\psi)$, namely

$$\mathcal{P}(\psi)\mathcal{F}(\psi) \quad (13)$$

$$\begin{aligned} &= \langle\psi|_B \left(\text{Tr}_{HH'} [|f(\psi)\rangle\langle f(\psi)|_{BHH'}] \right) |\psi\rangle_B \\ &\geq \langle\psi|_B \left(\text{Tr}_{HH'} [|\text{EPR}\rangle\langle \text{EPR}|_{HH'} \cdot |f(\psi)\rangle\langle f(\psi)|_{BHH'}] \right) |\psi\rangle_B \\ &= \langle\psi|_B \otimes \langle \text{EPR}|_{HH'} \left(|f(\psi)\rangle\langle f(\psi)|_{BHH'} \right) |\psi\rangle_B \otimes |\text{EPR}\rangle_{HH'} \\ &= \left| \langle\psi|_B \otimes \langle \text{EPR}|_{HH'} \cdot |f(\psi)\rangle_{BHH'} \right|^2. \end{aligned} \quad (14)$$

The above inequality holds because we also perform an EPR projective measurement on the joint system HH' before tracing them out. Next, by substituting Eq. (5) into Eq. (13), one obtains

$$\mathcal{P}(\psi)\mathcal{F}(\psi) \geq \left| \langle\psi|_B \otimes \langle \text{EPR}|_{AB'} \otimes \langle \text{EPR}|_{HH'} U_{AH} U_{B'H'}^* |\psi\rangle_A \otimes |\text{EPR}\rangle_{BB'} \otimes |\text{EPR}\rangle_{HH'} \right|^2. \quad (15)$$

Note that U_{AH} and $U_{B'H'}^*$ commute, and we can apply the equality given in Eq. (4) once more to replace $U_{B'H'}^*$ with U_{AH}^\dagger since

Thus, with $U_{AH}^\dagger U_{AH} = \mathbb{1}_{AH}$, Eq. (15) results in

$$\begin{aligned} \mathcal{P}(\psi)\mathcal{F}(\psi) &\geq \left| \langle\psi|_B \otimes \langle \text{EPR}|_{AB'} \cdot |\psi\rangle_A \otimes |\text{EPR}\rangle_{BB'} \right|^2 \\ &= \left| \frac{1}{\sqrt{d_A}} \frac{1}{\sqrt{d_A}} \sum_{i=0}^{d_A-1} \sum_{j=0}^{d_A-1} \langle i|\psi\rangle_A \cdot \langle \psi|j\rangle_B \cdot \langle i|j\rangle_{B'} \right|^2 \\ &= \left| \frac{1}{d_A} \sum_{i=0}^{d_A-1} \langle i|\psi\rangle \langle \psi|i \rangle \right|^2 \\ &= \frac{1}{d_A^2} \quad \forall \psi. \end{aligned} \quad (17)$$

We have completed the proof that a lower bound of $\mathcal{P}(\psi)\mathcal{F}(\psi)$ for an arbitrary initial state $|\psi\rangle$ is d_A^{-2} . ■

$$\begin{aligned} &\langle \text{EPR}|_{AB'} \otimes \langle \text{EPR}|_{HH'} \mathbb{1}_{AH} \otimes U_{B'H'}^* \\ &= \langle \text{EPR}|_{AB'} \otimes \langle \text{EPR}|_{HH'} U_{AH}^\dagger \otimes \mathbb{1}_{B'H'}. \end{aligned} \quad (16)$$

Directly observing QIS from the average success probability of the PCTC

Here, we show that the average success probability of the PCTC in our protocol equals to the average value of the OTOC (\mathcal{O}_{avg}). Note that a similar proof can also be found in Refs. [48, 76]. We begin by substituting Eq. (5) into Eq. (7) and averaging over all possible input states

ψ , namely

$$\begin{aligned} \int d\psi \mathcal{P}(\psi) &= \int d\psi \langle f(\psi) | f(\psi) \rangle \\ &= \int d\psi \langle \psi |_A \otimes \langle \text{EPR} |_{\text{BB}'} \otimes \langle \text{EPR} |_{\text{HH}'} \\ &\quad \times U_{\text{B}'\text{H}'}^T U_{\text{AH}}^\dagger | \text{EPR} \rangle \langle \text{EPR} |_{\text{AB}'} U_{\text{AH}} U_{\text{B}'\text{H}'}^* \\ &\quad \times | \psi \rangle_A \otimes | \text{EPR} \rangle_{\text{BB}'} \otimes | \text{EPR} \rangle_{\text{HH}'} \end{aligned} \quad (18)$$

Note that the above EPR projection operator $| \text{EPR} \rangle \langle \text{EPR} |_{\text{AB}'}$ can be represented as a Haar average over all local unitary operators W acting on the subsystems A and B' [48, 76]:

$$| \text{EPR} \rangle \langle \text{EPR} |_{\text{AB}'} = \int dW W_A \otimes W_{\text{B}'}^*. \quad (19)$$

Next, by substituting Eq. (19) into Eq. (18), one obtains

$$\begin{aligned} \int d\psi \mathcal{P}(\psi) &= \iint dW d\psi \langle \psi |_A \otimes \langle \text{EPR} |_{\text{BB}'} \otimes \langle \text{EPR} |_{\text{HH}'} U_{\text{B}'\text{H}'}^T U_{\text{AH}}^\dagger W_A W_{\text{B}'}^* U_{\text{AH}} U_{\text{B}'\text{H}'}^* | \psi \rangle_A \otimes | \text{EPR} \rangle_{\text{BB}'} \otimes | \text{EPR} \rangle_{\text{HH}'} \\ &= \iint dW d\psi \langle \psi |_A \otimes \langle \text{EPR} |_{\text{BB}'} \otimes \langle \text{EPR} |_{\text{HH}'} (U_{\text{B}'\text{H}'}^T W_{\text{B}'}^* U_{\text{B}'\text{H}'}^*) (U_{\text{AH}}^\dagger W_A U_{\text{AH}}) | \psi \rangle_A \otimes | \text{EPR} \rangle_{\text{BB}'} \otimes | \text{EPR} \rangle_{\text{HH}'} \\ &= \iint dW d\psi \langle \psi |_A \otimes \langle \text{EPR} |_{\text{BB}'} \otimes \langle \text{EPR} |_{\text{HH}'} (U_{\text{B}'\text{H}'}^\dagger W_{\text{B}'}^\dagger U_{\text{B}'\text{H}'})^T (U_{\text{AH}}^\dagger W_A U_{\text{AH}}) | \psi \rangle_A \otimes | \text{EPR} \rangle_{\text{BB}'} \otimes | \text{EPR} \rangle_{\text{HH}'} \\ &= \iint dW d\psi \langle \psi |_A \otimes \langle \text{EPR} |_{\text{BB}'} \otimes \langle \text{EPR} |_{\text{HH}'} (U_{\text{BH}}^\dagger W_{\text{B}'}^\dagger U_{\text{BH}}) (U_{\text{AH}}^\dagger W_A U_{\text{AH}}) | \psi \rangle_A \otimes | \text{EPR} \rangle_{\text{BB}'} \otimes | \text{EPR} \rangle_{\text{HH}'} \end{aligned} \quad (20)$$

Here, the last equality follows from Eq. (4). We can define the time-evolved version of W in the Heisenberg picture according to the scrambling unitary operator U , i.e., $W_A(t) = U_{\text{AH}}^\dagger W_A U_{\text{AH}}$ and $W_{\text{B}'}(t) = U_{\text{BH}}^\dagger W_{\text{B}'} U_{\text{BH}}$. Furthermore, the input state $| \psi \rangle_A$ can be generated by a unitary operator V acting on a fixed initial state $| \phi_0 \rangle_A$, i.e., $| \psi \rangle_A = V_A | \phi_0 \rangle_A$ and $V_A = | \psi \rangle \langle \phi_0 |_A$. Thus, the average over ψ can be performed by integrating over V , namely

$$\begin{aligned} \int d\psi \mathcal{P}(\psi) &= \iint dW dV \langle \phi_0 |_A \otimes \langle \text{EPR} |_{\text{BB}'} \otimes \langle \text{EPR} |_{\text{HH}'} \\ &\quad \times W_{\text{B}'}^\dagger(t) V_A^\dagger W_A(t) V_A \\ &\quad \times | \phi_0 \rangle_A \otimes | \text{EPR} \rangle_{\text{BB}'} \otimes | \text{EPR} \rangle_{\text{HH}'} \\ &= \iint dW dV \langle W_{\text{B}'}^\dagger(t) V_A^\dagger W_A(t) V_A | \\ &= \mathcal{O}_{\text{avg}}. \end{aligned} \quad (21)$$

This completes the proof that the average value of the OTOC (\mathcal{O}_{avg}) is equal to the average success probability of the PCTC in our protocol. ■

As discussed in the main text, we relabel certain systems to simplify the previous proof. To better illustrate

the connection between OTOCs and PCTCs through our decoding protocol, we revert to using the same labels and notations as in Fig. 1. Because the EPR projection operator is applied to the joint system EE' at T_2 [as shown in Fig. 2(a)], the unitary operator W in Eq. (19) should act on system E. Therefore, the OTOC $\langle W^\dagger(t) V^\dagger W(t) V \rangle$ in Eq. (21) can be interpreted as the overlap between the following two states:

$$\begin{aligned} W_E(t) V_A | \phi_0 \rangle_A \otimes | \text{EPR} \rangle_{\text{EE}'} \otimes | \text{EPR} \rangle_{\text{HH}'} \\ = U_{\text{HE} \rightarrow \text{BH}}^\dagger W_E U_{\text{AH} \rightarrow \text{HE}} V_A \\ \times | \phi_0 \rangle_A \otimes | \text{EPR} \rangle_{\text{EE}'} \otimes | \text{EPR} \rangle_{\text{HH}'}, \end{aligned} \quad (22)$$

$$\begin{aligned} V_A W_E(t) | \phi_0 \rangle_A \otimes | \text{EPR} \rangle_{\text{EE}'} \otimes | \text{EPR} \rangle_{\text{HH}'} \\ = V_A U_{\text{HE} \rightarrow \text{AH}}^\dagger W_E U_{\text{BH} \rightarrow \text{HE}} \\ \times | \phi_0 \rangle_B \otimes | \text{EPR} \rangle_{\text{EE}'} \otimes | \text{EPR} \rangle_{\text{HH}'}. \end{aligned} \quad (23)$$

The state in Eq. (22) follows the standard procedure of our protocol. Starting at T_1 , Alice prepares the state $| \psi \rangle_A$ by applying the unitary operator V_A on the initial state $| \phi_0 \rangle_A$, and then the information is encoded in the joint system HE at time T_2 by the encoding scrambler $U_{\text{AH} \rightarrow \text{HE}}$. A unitary operator W_E is then applied to system E, which can be regarded as a perturbation from

the perspective of QIS. After system E travels backward in time from T_2 to T_0 through the PCTC, the decoding operation $U_{\text{HE} \rightarrow \text{BH}}^\dagger$ is applied, and Bob receives the state.

In contrast, the state in Eq. (23) represents the inverse version of our protocol, where the direction of all timelines (as indicated by the arrows in Fig. 1) is reversed. As time proceeds backward from T_1 to T_0 , Bob encodes the state $|\phi_0\rangle_B$ into the joint system HE using the scrambling operation $(U_{\text{BH} \rightarrow \text{HE}}^\dagger)^\dagger = U_{\text{BH} \rightarrow \text{HE}}$. After system E travels forward in time from T_0 to T_2 through the PCTC, the perturbation W_E is applied to system E, and the temporal direction is again reversed at T_2 . As time proceeds backward from T_2 to T_1 , the decoding operation $U_{\text{HE} \rightarrow \text{AH}}^\dagger$ is applied, and Alice finally applies the unitary operator V_A to her state.

Consequently, the value of the OTOC for the specific unitary operators W_E and V_A can be determined by calculating the overlap between the output states from the standard and inverse versions of our decoding protocol. Nevertheless, for the average value of the OTOC (\mathcal{O}_{avg}), we highlight that it can be directly obtained from the average success probability of the PCTC in our decoding protocol using Eq. (21), without the need for the Haar averaging over all possible operators W_E and V_A .

ACKNOWLEDGMENTS

The authors acknowledge fruitful discussions with Chia-Yi Ju and Gelo Noel Tabia. The authors also acknowledge the NTU-IBM Q Hub, IBM Quantum, and Cloud Computing Center for Quantum Science & Technology at NCKU for providing us a platform to implement the experiments. YTH acknowledges the support of the National Science and Technology Council, Taiwan

(NSTC Grants No. 113-2917-I-006-024). A.M. was supported by the Polish National Science Centre (NCN) under the Maestro Grant No. DEC-2019/34/A/ST2/00081. GYC acknowledges the support of the National Science and Technology Council, Taiwan (NSTC Grants No. 113-2112-M-005-008). F.N. is supported in part by: the Japan Science and Technology Agency (JST) [via the CREST Quantum Frontiers program Grant No. JP-MJCR24I2, the Quantum Leap Flagship Program (Q-LEAP), and the Moonshot R&D Grant Number JP-MJMS2061], and the Office of Naval Research (ONR) Global (via Grant No. N62909-23-1-2074). YNC acknowledges the support of the National Center for Theoretical Sciences and the National Science and Technology Council, Taiwan (NSTC Grants No. 113-2123-M-006-001 and 114-2112-M-006 -015 -MY3).

AUTHOR CONTRIBUTIONS

Y.-T.H. conceived the research, carried out the theoretical analysis, performed the experiments with assistance from S.-W.H. and G.-Y.C., and wrote the manuscript under the supervision of Y.-N.C. J.-D.L., A.M., and N.L. provided critical input during manuscript preparation. Y.-N.C. and F.N. were responsible for integrating efforts across different research units. All authors contributed to discussions and interpretation of the results.

COMPETING INTERESTS

The authors declare no competing interests.

[1] S. Xu and B. Swingle, Scrambling Dynamics and Out-of-Time-Ordered Correlators in Quantum Many-Body Systems, *PRX Quantum* **5**, 010201 (2024).

[2] B. Swingle, Unscrambling the physics of out-of-time-order correlators, *Nat. Phys.* **14**, 988 (2018).

[3] E. Iyoda and T. Sagawa, Scrambling of quantum information in quantum many-body systems, *Phys. Rev. A* **97**, 042330 (2018).

[4] D. Ding, P. Hayden, and M. Walter, Conditional mutual information of bipartite unitaries and scrambling, *J. High Energy Phys.* **2016**, 145 (2016).

[5] N. Yunger Halpern, B. Swingle, and J. Dressel, Quasiprobability behind the out-of-time-ordered correlator, *Phys. Rev. A* **97**, 042105 (2018).

[6] S. Pappalardi, A. Russomanno, B. Žunković, F. Iemini, A. Silva, and R. Fazio, Scrambling and entanglement spreading in long-range spin chains, *Phys. Rev. B* **98**, 134303 (2018).

[7] A. Touil and S. Deffner, Quantum scrambling and the growth of mutual information, *Quantum Sci. Technol.* **5**, 035005 (2020).

[8] J.-D. Lin, W.-Y. Lin, H.-Y. Ku, N. Lambert, Y.-N. Chen, and F. Nori, Quantum steering as a witness of quantum scrambling, *Phys. Rev. A* **104**, 022614 (2021).

[9] K. K. Sharma and V. P. Gerdt, Quantum information scrambling and entanglement in bipartite quantum states, *Quantum Inf. Process.* **20**, 195 (2021).

[10] J. Harris, B. Yan, and N. A. Sinitzyn, Benchmarking Information Scrambling, *Phys. Rev. Lett.* **129**, 050602 (2022).

[11] Q. Zhu *et al.*, Observation of Thermalization and Information Scrambling in a Superconducting Quantum Processor, *Phys. Rev. Lett.* **128**, 160502 (2022).

[12] G. L. Monaco, L. Innocenti, D. Cilluffo, D. A. Chisholm, S. Lorenzo, and G. M. Palma, An operational definition of quantum information scrambling, [arXiv:2312.11619](https://arxiv.org/abs/2312.11619) (2023).

[13] R. J. Garcia, K. Bu, and A. Jaffe, Resource theory of quantum scrambling, *Proc. Natl. Acad. Sci.* **120**, e2217031120 (2023).

[14] P. Hosur, X.-L. Qi, D. A. Roberts, and B. Yoshida, Chaos in quantum channels, *J. High Energy Phys.* **2016**, 4

(2016).

[15] A. Seshadri, V. Madhok, and A. Lakshminarayanan, Tripartite mutual information, entanglement, and scrambling in permutation symmetric systems with an application to quantum chaos, *Phys. Rev. E* **98**, 052205 (2018).

[16] N. Dowling, P. Kos, and K. Modi, Scrambling Is Necessary but Not Sufficient for Chaos, *Phys. Rev. Lett.* **131**, 180403 (2023).

[17] J. Maldacena and D. Stanford, Remarks on the Sachdev-Ye-Kitaev model, *Phys. Rev. D* **94**, 106002 (2016).

[18] A. Nahum, J. Ruhman, S. Vijay, and J. Haah, Quantum entanglement growth under random unitary dynamics, *Phys. Rev. X* **7**, 031016 (2017).

[19] C. W. von Keyserlingk, T. Rakovszky, F. Pollmann, and S. L. Sondhi, Operator hydrodynamics, OTOCs, and entanglement growth in systems without conservation laws, *Phys. Rev. X* **8**, 021013 (2018).

[20] J. Cotler, N. Hunter-Jones, J. Liu, and B. Yoshida, Chaos, complexity, and random matrices, *J. High Energy Phys.* **2017**, 48 (2017).

[21] R. Fan, P. Zhang, H. Shen, and H. Zhai, Out-of-time-order correlation for many-body localization, *Sci. Bull.* **62**, 707 (2017).

[22] Y. Gu, X.-L. Qi, and D. Stanford, Local criticality, diffusion and chaos in generalized Sachdev-Ye-Kitaev models, *J. High Energy Phys.* **2017**, 125 (2017).

[23] V. Khemani, A. Vishwanath, and D. A. Huse, Operator spreading and the emergence of dissipative hydrodynamics under unitary evolution with conservation laws, *Phys. Rev. X* **8**, 031057 (2018).

[24] M. Zonnios, J. Levinsen, M. M. Parish, F. A. Pollock, and K. Modi, Signatures of Quantum Chaos in an Out-of-Time-Order Tensor, *Phys. Rev. Lett.* **128**, 150601 (2022).

[25] M. Tezuka, O. Oktay, E. Rinaldi, M. Hanada, and F. Nori, Binary-coupling sparse Sachdev-Ye-Kitaev model: An improved model of quantum chaos and holography, *Phys. Rev. B* **107**, L081103 (2023).

[26] Q. Bin, L.-L. Wan, F. Nori, Y. Wu, and X.-Y. Lü, Out-of-time-order correlation as a witness for topological phase transitions, *Phys. Rev. B* **107**, L020202 (2023).

[27] J. R. G. Alonso, N. Shammah, S. Ahmed, F. Nori, and J. Dressel, Diagnosing quantum chaos with out-of-time-ordered-correlator quasiprobability in the kicked-top model, [arXiv:2201.08175](https://arxiv.org/abs/2201.08175) (2022).

[28] P. Hayden and J. Preskill, Black holes as mirrors: Quantum information in random subsystems, *J. High Energy Phys.* **2007**, 120 (2007).

[29] Y. Sekino and L. Susskind, Fast scramblers, *J. High Energy Phys.* **2008**, 065 (2008).

[30] N. Lashkari, D. Stanford, M. Hastings, T. Osborne, and P. Hayden, Towards the fast scrambling conjecture, *J. High Energy Phys.* **2013**, 22 (2013).

[31] S. H. Shenker and D. Stanford, Black holes and the butterfly effect, *J. High Energy Phys.* **2014**, 67 (2014).

[32] D. A. Roberts and D. Stanford, Diagnosing chaos using four-point functions in two-dimensional conformal field theory, *Phys. Rev. Lett.* **115**, 131603 (2015).

[33] M. Blake, Universal charge diffusion and the butterfly effect in holographic theories, *Phys. Rev. Lett.* **117**, 091601 (2016).

[34] P. Gao, D. L. Jafferis, and A. C. Wall, Traversable wormholes via a double trace deformation, *J. High Energy Phys.* **2017**, 151 (2017).

[35] J. Maldacena, D. Stanford, and Z. Yang, Diving into traversable wormholes, *Fortschr. Phys.* **65**, 1700034 (2017).

[36] B. Chen, B. Czech, and Z.-Z. Wang, Quantum information in holographic duality, *Rep. Prog. Phys.* **85**, 046001 (2022).

[37] J. Liu, Scrambling and decoding the charged quantum information, *Phys. Rev. Res.* **2**, 043164 (2020).

[38] E. Rinaldi, X. Han, M. Hassan, Y. Feng, F. Nori, M. McGuigan, and M. Hanada, Matrix-Model Simulations Using Quantum Computing, Deep Learning, and Lattice Monte Carlo, *PRX Quantum* **3**, 010324 (2022).

[39] P. D. Nation, M. P. Blencowe, and F. Nori, Non-equilibrium Landauer transport model for Hawking radiation from a black hole, *New J. Phys.* **14**, 033013 (2012).

[40] Y. Li, X. Li, and J. Jin, Information scrambling in a collision model, *Phys. Rev. A* **101**, 042324 (2020).

[41] Y. Li, X. Li, and J. Jin, Dissipation-Induced Information Scrambling in a Collision Model, *Entropy* **24**, 345 (2022).

[42] F. Tian, J. Zou, H. Li, L. Han, and B. Shao, Relationship between Information Scrambling and Quantum Darwinism, *Entropy* **26**, 19 (2024).

[43] H. Shen, P. Zhang, Y.-Z. You, and H. Zhai, Information Scrambling in Quantum Neural Networks, *Phys. Rev. Lett.* **124**, 200504 (2020).

[44] S. Choi, Y. Bao, X.-L. Qi, and E. Altman, Quantum Error Correction in Scrambling Dynamics and Measurement-Induced Phase Transition, *Phys. Rev. Lett.* **125**, 030505 (2020).

[45] Z. Li, H. Zheng, Y. Wang, L. Jiang, Z.-W. Liu, and J. Liu, SU(d)-Symmetric random unitaries: Quantum scrambling, error correction, and machine learning, [arXiv:2309.16556](https://arxiv.org/abs/2309.16556) (2023).

[46] B. Yan and N. A. Sinitzyn, Recovery of Damaged Information and the Out-of-Time-Ordered Correlators, *Phys. Rev. Lett.* **125**, 040605 (2020).

[47] B. Yoshida and A. Kitaev, Efficient decoding for the Hayden-Preskill protocol, [arXiv:1710.03363](https://arxiv.org/abs/1710.03363) (2017).

[48] B. Yoshida and N. Y. Yao, Disentangling Scrambling and Decoherence via Quantum Teleportation, *Phys. Rev. X* **9**, 011006 (2019).

[49] N. Bao and Y. Kikuchi, Hayden-Preskill decoding from noisy Hawking radiation, *J. High Energy Phys.* **2021**, 17 (2021).

[50] T. Schuster, B. Kobrin, P. Gao, I. Cong, E. T. Khabit-bouline, N. M. Linke, M. D. Lukin, C. Monroe, B. Yoshida, and N. Y. Yao, Many-Body Quantum Teleportation via Operator Spreading in the Traversable Wormhole Protocol, *Phys. Rev. X* **12**, 031013 (2022).

[51] K. A. Landsman, C. Figgatt, T. Schuster, N. M. Linke, B. Yoshida, N. Y. Yao, and C. Monroe, Verified quantum information scrambling, *Nature (London)* **567**, 61 (2019).

[52] M. S. Blok, V. V. Ramasesh, T. Schuster, K. O'Brien, J. M. Kreikebaum, D. Dahmen, A. Morvan, B. Yoshida, N. Y. Yao, and I. Siddiqi, Quantum Information Scrambling on a Superconducting Qutrit Processor, *Phys. Rev. X* **11**, 021010 (2021).

[53] J.-H. Wang *et al.*, Information scrambling dynamics in a fully controllable quantum simulator, *Phys. Rev. Res.* **4**, 043141 (2022).

[54] I. Shapoval, V. P. Su, W. de Jong, M. Urbanek, and B. Swingle, Towards Quantum Gravity in the Lab on Quantum Processors, *Quantum* **7**, 1138 (2023).

[55] S. Lloyd, L. Maccone, R. Garcia-Patron, V. Giovannetti, Y. Shikano, S. Pirandola, L. A. Rozema, A. Darabi, Y. Soudagar, L. K. Shalm, and A. M. Steinberg, Closed timelike curves via postselection: Theory and experimental test of consistency, *Phys. Rev. Lett.* **106**, 040403 (2011).

[56] S. Lloyd, L. Maccone, R. Garcia-Patron, V. Giovannetti, and Y. Shikano, Quantum mechanics of time travel through post-selected teleportation, *Phys. Rev. D* **84**, 025007 (2011).

[57] W. J. van Stockum, The gravitational field of a distribution of particles rotating about an axis of symmetry, *Proc. R. Soc. Edinb.* **57**, 135–154 (1938).

[58] K. Gödel, An example of a new type of cosmological solutions of Einstein’s field equations of gravitation, *Rev. Mod. Phys.* **21**, 447 (1949).

[59] M. S. Morris, K. S. Thorne, and U. Yurtsever, Wormholes, time machines, and the weak energy condition, *Phys. Rev. Lett.* **61**, 1446 (1988).

[60] I. Buluta and F. Nori, Quantum Simulators, *Science* **326**, 108 (2009).

[61] I. M. Georgescu, S. Ashhab, and F. Nori, Quantum simulation, *Rev. Mod. Phys.* **86**, 153 (2014).

[62] P. D. Nation, J. R. Johansson, M. P. Blencowe, and F. Nori, *Colloquium*: Stimulating uncertainty: Amplifying the quantum vacuum with superconducting circuits, *Rev. Mod. Phys.* **84**, 1 (2012).

[63] J. Friedman, M. S. Morris, I. D. Novikov, F. Echeverria, G. Klinkhammer, K. S. Thorne, and U. Yurtsever, Cauchy problem in spacetimes with closed timelike curves, *Phys. Rev. D* **42**, 1915 (1990).

[64] S. Lloyd and J. Preskill, Unitarity of black hole evaporation in final-state projection models, *J. High Energy Phys.* **2014**, 126 (2014).

[65] P. Xu *et al.*, Satellite testing of a gravitationally induced quantum decoherence model, *Science* **366**, 132–135 (2019).

[66] I. H. Kim and J. Preskill, Complementarity and the unitarity of the black hole s-matrix, *J. High Energy Phys.* **2023**, 233 (2023).

[67] O. Oreshkov and N. J. Cerf, Operational formulation of time reversal in quantum theory, *Nat. Phys.* **11**, 853–858 (2015).

[68] S. M. Korotaev and E. O. Kiktenko, Quantum causality in closed timelike curves, *Phys. Scr.* **90**, 085101 (2015).

[69] G. Chiribella and Z. Liu, Quantum operations with indefinite time direction, *Commun. Phys.* **5**, 190 (2022).

[70] E. O. Kiktenko, Exploring postselection-induced quantum phenomena with time-bidirectional state formalism, *Phys. Rev. A* **107**, 032419 (2023).

[71] D. R. M. Arvidsson-Shukur, A. G. McConnell, and N. Yunger Halpern, Nonclassical advantage in metrology established via quantum simulations of hypothetical closed timelike curves, *Phys. Rev. Lett.* **131**, 150202 (2023).

[72] X. Song, F. Salvati, C. Gaikwad, N. Yunger Halpern, D. R. M. Arvidsson-Shukur, and K. Murch, Agnostic phase estimation, *Phys. Rev. Lett.* **132**, 260801 (2024).

[73] Quantinuum H1-1, <https://www.quantinuum.com/>, (2024).

[74] M. A. Nielsen and I. L. Chuang, *Quantum Computation and Quantum Information: 10th Anniversary Edition* (Cambridge University Press, 2012).

[75] M. Pawłowski, T. Paterek, D. Kaszlikowski, V. Scarani, A. Winter, and M. Żukowski, Information causality as a physical principle, *Nature* **461**, 1101 (2009).

[76] D. A. Roberts and B. Yoshida, Chaos and complexity by design, *J. High Energy Phys.* **2017**, 121 (2017).

Supplementary Information to “Decoding scrambled quantum information that was never encoded: An experimental demonstration”

Yi-Te Huang,^{1, 2, 3} Siang-Wei Huang,^{1, 2} Jhen-Dong Lin,^{1, 2} Adam Miranowicz,^{3, 4}
Neill Lambert,³ Guang-Yin Chen,⁵ Franco Nori,^{3, 6, *} and Yueh-Nan Chen^{1, 2, 7, †}

¹*Department of Physics, National Cheng Kung University, Tainan 701401, Taiwan*

²*Center for Quantum Frontiers of Research and Technology (QFort), Tainan 701401, Taiwan*

³*RIKEN Center for Quantum Computing, RIKEN, Wakoshi, Saitama 351-0198, Japan*

⁴*Institute of Spintronics and Quantum Information, Faculty of Physics and Astronomy,
Adam Mickiewicz University, 61-614 Poznań, Poland*

⁵*Department of Physics, National Chung Hsing University, Taichung 402202, Taiwan*

⁶*Physics Department, The University of Michigan, Ann Arbor, Michigan 48109-1040, USA.*

⁷*Physics Division, National Center for Theoretical Sciences, Taipei 106319, Taiwan*

(Dated: July 29, 2025)

Introduction

Our findings presented in the main text illuminate the interplay between quantum information scrambling (QIS) and the concept of postselected closed timelike curves (PCTCs) in quantum mechanics, offering a fresh perspective on accessing globally encoded information in a quantum system at earlier times without altering the past. Key contributions of our study include:

- Theoretical framework: We propose a protocol leveraging postselected closed timelike curves to enable the decoding even before the original information is generated.
- Scrambling dynamics: We demonstrate that stronger QIS enhances the decoding fidelity.
- Estimating out-of-time-order correlators (OTOCs): Our protocol enables the estimation of the averaged OTOC for arbitrary QIS dynamics using only one additional entangled EPR pair.
- Experimental validation: Our protocol is implemented and validated on a Quantinuum trapped-ion quantum processor called H1-1, demonstrating its feasibility and the critical role of scrambling dynamics in achieving high decoding fidelity.

This work builds on foundational concepts in quantum mechanics, including QIS, OTOCs, and PCTCs. By bridging these ideas, our study contributes to the understanding of quantum information processing and its relationship to time and causality, with potential implications for quantum error correction, quantum gravity, and fundamental physics.

In this Supplementary Information, we conduct the experiment described in the main text on an IBM Quantum processor called *ibm_torino* with two different Clifford scrambling unitary dynamics. Furthermore, we present the calibration data of both Quantinuum H1-1 and IBM *ibm_torino* quantum processors.

Calibration data for the Quantinuum processor

In the main text, we performed the experiment on the Quantinuum H1-1 quantum charge-coupled processor, which features 20 trapped-ion ($^{171}\text{Yb}^+$) qubits with all-to-all connectivity [1]. This allows the circuit given in the main text to be executed directly on the H1-1 processor. The calibration data for H1-1 is presented in Table S1.

* fnori@riken.jp

† yuehnan@mail.ncku.edu.tw

TABLE S1. Calibration data (obtained on Apr. 10, 2024) for the Quantinuum processor H1-1 used in our experiments.

Relaxation time	$\gg 1$ minute
Decoherence time	≈ 4 seconds
Readout error	2.5×10^{-3}
Single-qubit gate error	2.1×10^{-5}
Two-qubit gate error	8.8×10^{-4}

Experimental results obtained from the IBM Quantum processor using different scrambling unitary operators

We also conducted the experiment described in the main text on an IBM Quantum processor called *ibm_torino*, which contains 133 superconducting qubits [2, 3]. The topology of the qubits used in the experiment is illustrated in Fig. S2(a), and the corresponding calibration data for each used qubit is presented in Table S2.

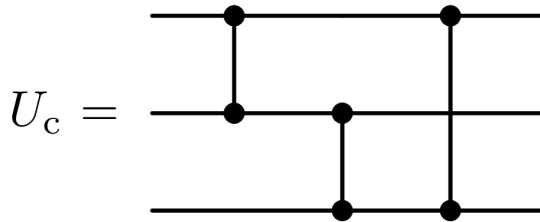
TABLE S2. Calibration data (obtained on Sep. 26, 2024) for the IBM Quantum processor *ibm_torino* used in our experiments. The qubit index refer to those in Fig. S2(a). Here, R_Z is a single-qubit rotation gate around the Z -axis, and \sqrt{X} is the square root of Pauli- X gate. The average two-qubit (controlled- Z) gate error is estimated to be 1.62×10^{-3} .

System label (at time T_0)	Qubit index	Relaxation time (μ s)	Decoherence time (μ s)	Frequency (GHz)	Anharmonicity (GHz)	Errors		
						Readout	R_Z	\sqrt{X}
H	87	293.88	256.22	0	0	6.30×10^{-3}	0	1.44×10^{-4}
	88	280.95	403.23	0	0	2.54×10^{-2}	0	1.49×10^{-4}
E	94	274.41	272.24	0	0	1.07×10^{-2}	0	1.52×10^{-4}
E'	107	88.68	105.80	0	0	2.86×10^{-2}	0	5.16×10^{-4}

Additionally, to show the strength of U_q in the main text, we compare it with another Clifford scrambler, denoted as U_c , which only scrambles classical information [4]. The explicit matrix form of this unitary operator is given by:

$$U_c = \text{diag}(1, 1, 1, -1, 1, -1, -1, -1), \quad (1)$$

and its circuit representation is given in Fig. S1. In this case, the average success probability of the PCTC $\mathcal{P}_{\text{avg}} = 0.5$, resulting in a lower bound on the fidelity of 0.5, due to Eq. (8) in the main text. Only states $|\psi\rangle$ prepared in $|0\rangle$ or $|1\rangle$ can be perfectly decoded, while the fidelity of all other states is 0.5.

FIG. S1. Circuit representation of the three-qubit Clifford classical information scrambler. This scrambling unitary operator includes three controlled- Z gates.

However, the two-qubit gates in the circuit representations of U_q (given in Fig. 4 in the main text) and U_c (given in Fig. S1) do not match the topology shown in Fig. S2(a). Therefore, we provide circuit decompositions in Fig. S2(b) and Fig. S2(c) to align with the topology of *ibm_torino*, and the corresponding decomposition of each Hadamard gate is shown in Fig. S2(d).

The experimental results, as shown in Table S3, are obtained through 40,000 shots for each measurement procedure in the state tomography using the *ibm_torino*. When U_q is employed as the scrambler in the protocol, we observe that the success probability $\mathcal{P}(\psi)$ of time travel approximately approaches $d_A^{-2} = 0.25$ for all initial states $|\psi\rangle$, which also means that $\mathcal{O}_{\text{avg}} \approx 0.25$ due to Eq. (10) in the main text. Due to the strong QIS U_q , the decoding protocol succeeds with an average fidelity of 0.8453. Additionally, it can be observed that the average fidelity achieved on the H1-1 processor (as shown in Table I in the main text) is higher than that on *ibm_torino*. This is attributed to the H1-1

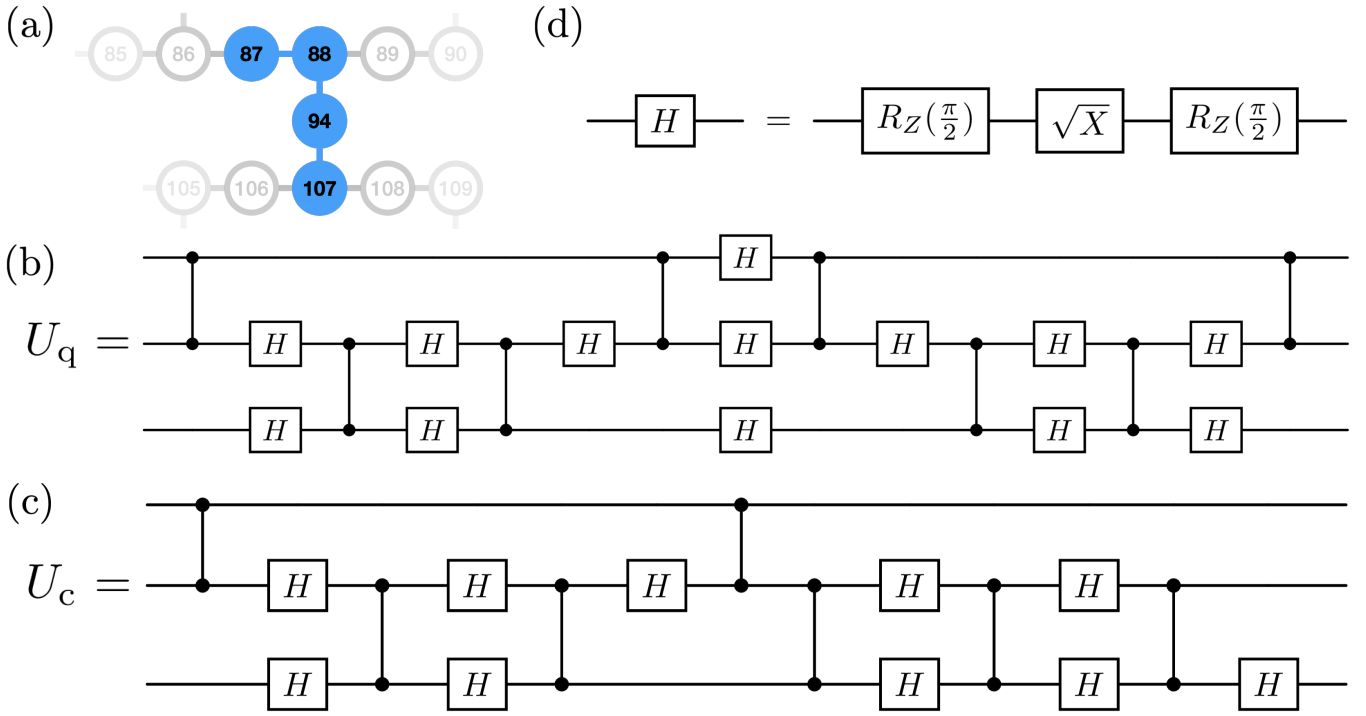


FIG. S2. Topology of the IBM Quantum processor (*ibm_torino*) and circuit decompositions used. (a) Topology of the *ibm_torino* where the blue solid circles are the qubits used to conduct the experiment. (b) Circuit decomposition of the Clifford quantum information scrambler U_q for *ibm_torino*. (c) Circuit decomposition of the Clifford classical information scrambler U_c for *ibm_torino*. (d) The circuit decomposition of each Hadamard gate H is given by a single \sqrt{X} gate and two R_Z (rotation around the Z -axis) gates with the rotational angle $\pi/2$.

TABLE S3. Experimental results obtained from the IBM Quantum processor. The decoding fidelity \mathcal{F} and the success probability \mathcal{P} of time travel for different initial states $|\psi\rangle$ under Clifford scramblers (U_q and U_c). As shown in Eq. (10) in the main text, the average value of the out-of-time-order correlator \mathcal{O}_{avg} equals the average value of $\mathcal{P}(\psi)$. Note that these results can be substantially improved—reaching fidelities comparable to those reported by Quantinuum in the main text—through the use of advanced error mitigation techniques developed by Algoritmique [5].

$ \psi\rangle$	$ x_-\rangle$	$ x_+\rangle$	$ y_-\rangle$	$ y_+\rangle$	$ z_-\rangle$	$ z_+\rangle$	Average	
U_q	$\mathcal{F}(\psi)$	0.8320	0.8219	0.8681	0.8506	0.8479	0.8512	0.8453
	$\mathcal{P}(\psi)$	0.2519	0.2619	0.2592	0.2578	0.2566	0.2564	0.2573
U_c	$\mathcal{F}(\psi)$	0.5021	0.5014	0.4949	0.5082	0.9092	0.9130	0.6381
	$\mathcal{P}(\psi)$	0.4430	0.4440	0.4454	0.4406	0.4405	0.4461	0.4433

processor's longer qubit relaxation and decoherence times, as well as lower readout and gate error rates (see Tables S1 and S2 for the calibration data of both processors).

In contrast, applying the same protocol with the scrambler U_c using *ibm_torino* results in a low decoding fidelity. Although the fidelity for states $|z_{\pm}\rangle$ remains relatively high (around 0.91), the fidelity drops significantly to around 0.5 for other states ($|x_{\pm}\rangle$ and $|y_{\pm}\rangle$). This indicates that U_c only has the capability to scramble classical information ($|z_{\pm}\rangle$) instead of general quantum information. The large value of $\mathcal{O}_{\text{avg}} = \mathcal{P}_{\text{avg}} = 0.4433$ further supports this conclusion.

[1] Quantinuum H1-1, <https://www.quantinuum.com/>, (2024).
 [2] IBM Quantum, <https://quantum.ibm.com/>, (2021).
 [3] A. Javadi-Abhari *et al.*, Quantum computing with Qiskit, [arXiv:2405.08810](https://arxiv.org/abs/2405.08810) (2024).
 [4] B. Yoshida and N. Y. Yao, Disentangling Scrambling and Decoherence via Quantum Teleportation, *Phys. Rev. X* **9**, 011006 (2019).

[5] Private communication, discussion with Keijo Korhonen, Matteo Rossi, Sergei Filippov, and Sabrina Maniscalco from Algorithmiq, May 2025.